


## The exceptional preservation of Aix-en-Provence spider fossils could have been facilitated by diatoms

Alison N. Olcott <sup>1</sup>, Matthew R. Downen<sup>1</sup>, James D. Schiffbauer <sup>2,3</sup> & Paul A. Selden <sup>1,4</sup>

Much of our understanding of the history of life on Earth comes from fossil sites with exceptional preservation. Here, we use microscopy and chemical analysis of spiders found in the Oligocene Aix-en-Provence Formation, France, to unravel the taphonomic pathway responsible for the preservation of these arachnids. Microscopy revealed the presence of diatom mats and a black polymer on the body of the spiders, while elemental analysis revealed the polymer was composed of co-localized carbon and sulfur. We hypothesize that the extracellular polymeric substances produced by the diatoms found widely in this deposit could have helped promote the sulfurization of the spiders. Additionally, examination of similar Fossil-Lagerstätten reveals that this preservation pathway may be widespread across the Cenozoic and, if so, would be responsible for much of our understanding of insect, arachnid, amphibian, and plant life preserved in lacustrine settings.

<sup>1</sup> Department of Geology, University of Kansas, Lawrence, KS 66045, USA. <sup>2</sup> Department of Geological Sciences, University of Missouri, Columbia, MO 65211, USA. <sup>3</sup> X-ray Microanalysis Core, University of Missouri, Columbia, MO 65211, USA. <sup>4</sup> Natural History Museum, London SW7 5BD, UK.

email: [olcott@ku.edu](mailto:olcott@ku.edu)

The vast majority of fossils are originally made of bio-synthesized minerals like calcite and apatite<sup>1</sup>. Mineralized body parts, like shells, bones, and teeth, have a relatively straightforward pathway to preservation. On the other hand, soft tissues composed of carbonaceous polymers, like chitinous exoskeletons, skin, and feathers, are much less likely to fossilize. Unlike mineralized hard parts, these materials are more likely to decay than be preserved once an organism dies. As a result, these types of organisms and body parts are underrepresented in the fossil record and are often found only in cases of exceptional preservation<sup>1</sup>. These deposits, also called Fossil-Lagerstätten, tend to be the result of specific taphonomic pathways that allow the soft tissues to be preserved before the onset of the rapid process of decay<sup>1–3</sup>. Although these types of deposits are relatively rare, they provide a much more complete view of ancient life, as they preserve a representative view of an ancient environment, rather than just the biomineralized organisms in that environment<sup>4</sup>. Given their importance, understanding the chemical pathways that promote this exceptional preservation can help to both elucidate the paleoenvironmental setting where they occur, and also serve as a guide to find more of such deposits.

There has not been a sustained focus on the taphonomic pathways of a series of exceptionally preserved Cenozoic insect and arachnid deposits<sup>5</sup>. Some individual units have been studied, for example with focuses on the Eocene Florissant Formation in Colorado, the Oligocene Canyon Ferry deposit in Montana, the Miocene Stewart Valley and Savage Canyon Formations, Nevada, the Miocene Shanwang Beds in Shandong Province, northeast China, and a Miocene deposit near Tresjuncos, Spain<sup>6–8</sup>. These studies all noted that well-preserved fossils are covered in diatom mats and hypothesized that the extracellular polymeric substances (EPS) associated with these mats would have produced an anaerobic environment that would have slowed bacterial decay processes, allowing for the preservation of the fossils. However, this model fails to explain why microbialites, including ones in correlative sections, fail to preserve such an extensive variety of fossil biota. If the presence of EPS alone was enough to induce exquisite preservation, then bacterial mats should also provide a similar taphonomic pathway, as bacteria produce as much EPS as diatoms<sup>9</sup>.

In order to better understand the taphonomic pathways that led to this plausibly diatom-influenced exceptional preservation, we performed chemical and microscopic analyses of fossil spiders from the Oligocene Aix-en-Provence Formation in France. This paired approach reveals details about the preservation of these arachnids. The chemical analyses reveal that the spider fossils are preserved as carbonaceous films while microscopic characterization reveals that the spider fossils are surrounded and covered by diatoms, a microfossil never before reported from Aix-en-Provence Formation. The co-localization of the fossils and the chemical composition suggests that this extraordinary preservation is not merely due to the fact that diatom EPS induces an anaerobic environment. Instead, we hypothesize that the chemical composition of the diatom EPS is such that it reacts with the organic polymers present in the organism, inducing polymerization of the original organic material and leading to this exceptional preservation. In addition, we demonstrate that this mode of preservation is much more widespread than previously known, as the majority of the exceptionally preserved fossil deposits across the Cenozoic occur in diatom-rich units. Thus, the chemical reactions induced by the diatom mats are responsible for much of our understanding of Cenozoic paleoecology and paleontology.

## Diatoms

Diatoms (Bacillariophyceae) are siliceous photosynthetic microalgae that first appear in the fossil record during late Jurassic with

an estimated origin closer to the Triassic<sup>10–13</sup>. Although there are some reports of lacustrine diatoms in the Late Cretaceous<sup>13</sup>, it was not until the middle Eocene that they became abundant in the continental realm<sup>10–13</sup>. A series of post-Cretaceous sea level rises introduced the siliceous microalgae into lacustrine environments, then influxes of silica from volcanism and the expansion of grasslands throughout the Paleogene resulted in the spread and evolution of lacustrine diatoms<sup>14,15</sup>. Terrestrial diatoms experienced an evolutionary turnover and expansion in the middle/Late Miocene<sup>16</sup>, while marine diatoms reached peak diversity at the Eocene/Oligocene boundary<sup>17</sup>. As a result of these expansions, the Cenozoic as a whole is marked by a high abundance of globally distributed diatomite deposits<sup>18</sup>.

These microalgae are single-celled organisms encased in two ornamented silica valves<sup>19</sup>. Diatoms have two general morphologies: pennate, which are bilaterally symmetric, and centric, which are radially symmetric. Both types of diatoms can excrete EPS, and nearshore pennate diatoms, in particular, can excrete large quantities<sup>20</sup>. Diatoms generate three types of EPS: one is found as a coating around the cell, one is a soluble form thought to aid in motility, and one, also known as transparent exopolymeric particles, forms sheets or strings as long as 100  $\mu\text{m}$ <sup>21,22</sup>. The soluble form of EPS is found in great quantities in diatom mats, and diatom EPS and transparent exopolymeric particles comprise a large proportion of the material in marine snow, helping to package and transport organic carbon down to the seafloor quickly<sup>21</sup>. The same is true in lacustrine settings, as limnetic aggregates (lake snow) form from the flocculation of diatoms and have fast sinking rates<sup>23,24</sup>.

Chemically, the three types of diatom EPS have been found to be 40–90% carbohydrates<sup>25</sup>, and these carbohydrates are often sulfated or contain sulfonate esters<sup>26,27</sup>. This sulfate can make up a large proportion of the total mass of the EPS; one study found that up to 30 wt% of the polymers are sulfated<sup>22,28,29</sup>. Although some photosynthetic algae have been found to produce chemically similar EPS, this chemical composition distinguishes the EPS produced by diatoms from that made by bacteria. Bacterial EPS is composed primarily of polysaccharides as well, but sulfate compounds have not been identified within the matrix of bacterial EPS<sup>9</sup>, except within Arctic and hydrothermal vent bacteria<sup>30</sup>. Although many researchers have considered diatom EPS and bacterial EPS to be interchangeable<sup>31</sup>, chemically they are quite distinct.

## Geological setting

The Aix-en-Provence Formation of France contains an abundance of fossil fish, plants, and terrestrial arthropods preserved as compression fossils<sup>32</sup>. Dated to 22.5 Ma, the Aix-en-Provence Formation consists of a 150 m succession of informally named subunits<sup>33,34</sup>. The unit is mainly composed of marlstones and gypsum, indicating an evaporative environment, although there is some debate over whether these rocks were deposited in a lacustrine or brackish lagoonal setting<sup>34,35</sup>. The fossils are found in the unit often referred to as the Insect Bed, which, in turn, is part of the informal Calcaires et marnes à gypse d'Aix (Aix limestones and gypsum marls)<sup>33,34,36</sup>. The Insect Bed is roughly 80 cm in thickness and represented by laminated light gray and light green calcareous marlstone; the original locality was destroyed in the 1970s. The laminations are extremely thin, laterally continuous over 6 km and contain no reported trace fossils or bioturbation, although they do contain a wide variety of fossils, including insects, fish, and shrimp<sup>34</sup>. Study of this fossil biota began in the late 1700s and continues to this day, but little research has focused on the taphonomic processes and pathways responsible for the exceptional preservation in this deposit<sup>33,34</sup>.

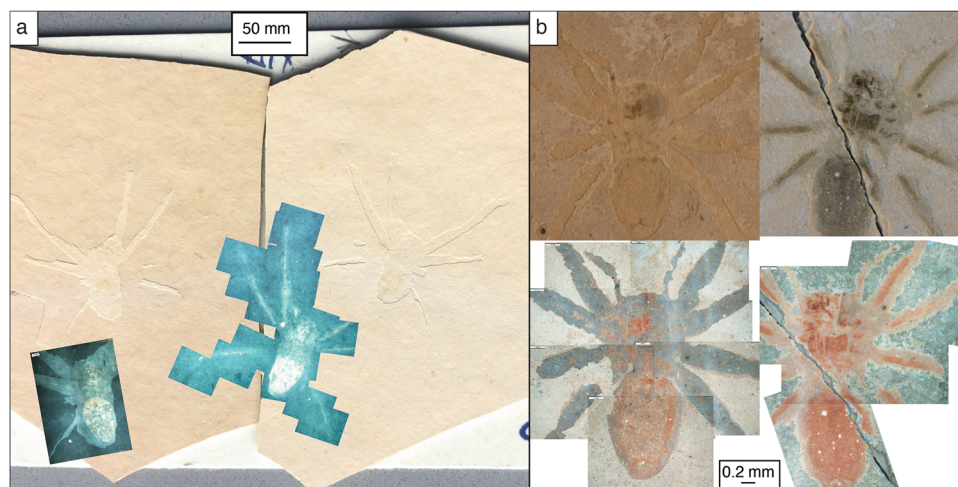


**Fig. 1** Part and counterpart of two fossil spiders shown in plain light and under UV illumination. Fossils Aix\_25 (**a**) and Aix\_17 (**b**), shown in plain light and under UV illumination. In plain light, the fossils do not contain many discernible details, but under UV illumination, the autofluorescence reveals additional detail, as areas of the spider autofluoresce yellow (**a**) and red (**b**).

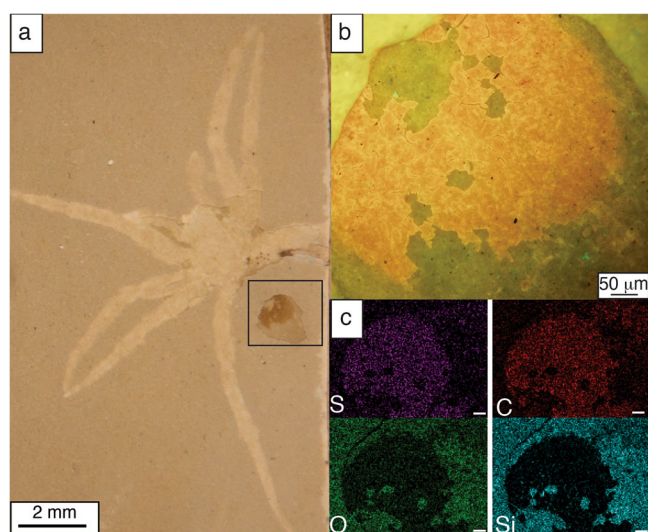


**Fig. 2** Fossil spider shown in plain light, with abdomen illuminated by UV light and analyzed by energy-dispersive x-ray spectroscopy. **a** Aix\_Flat 1 shown in plain light, which does not reveal many details on the fossil. **b** Spider abdomen (area in box in **a**) under UV illumination. The material that is dark under plain light autofluoresces orange, revealing a cracked polymer overlaying the matrix. **c** Elemental maps revealing the composition of this polymer, revealing that it is composed of C and S, while the surrounding matrix contains Si and O. All scale bars in panel **c** are 100  $\mu\text{m}$ .

## Results

**Fluorescent microscopy.** In hand sample, there is relatively low contrast between the fossils and the surrounding matrix (Fig. 1). The fossils preserve the general habitus of the organism, but morphological details are generally not discernible. However, some of the fossils preserve a dark brown material within the body of the spider (Figs. 1b and 2a). When fossils are preserved as part and counterpart, material is found only on one half or the other at any given location on the fossil (Fig. 1b).

Despite this lack of contrast under visible light, when illuminated with UV (330–385 nm wavelength) light, the fossils and the surrounding matrix exhibit a strong autofluorescent response. The fossils fluoresce yellow (Fig. 1a) or orange, with the orange corresponding to areas that appear brown under plane-polarized light (Figs. 1b and 2a, b). In many cases, the autofluorescent

responses evidenced by the fossil reveal extra morphological details such as pedipalps, claws, and setal structures that are important taxonomic features (Fig. 3). Additionally, the autofluorescence reveals more details about the dark brown material, showing it to be a cohesive material that has cracked and flaked off in places (Fig. 2b).

Autofluorescence reveals extra details in the matrix, as well. In plane view, the matrix surrounding the fossils fluoresces yellow or blue (Figs. 1 and 2b). Petrographic 30  $\mu\text{m}$ -thick thin sections made perpendicular to the matrix reveal alternating green and yellow extremely fine (10–50  $\mu\text{m}$ ) laminae under UV illumination (Fig. 4a). These thin sections also reveal the presence of microfossils throughout the matrix. Under brightfield illumination, the thin sections reveal clear objects, about 10  $\mu\text{m}$  long with a discernable spot; under UV illumination that spot shows a red autofluorescent response (Fig. 4b).

**Scanning electron microscopy.** SEM imaging of the fossils reveals that the dark material that covers the fossils is seen to be a black (low atomic number) material that drapes over the matrix (Fig. 5a–d). This material appears very cohesive, and even preserves impressions of fine morphological details of the cuticle, including spine-like macrosetae on the legs (Fig. 5d at white arrow). SEM also reveals numerous types of microfossils associated with all the specimens: small (15–20  $\mu\text{m}$ ) hollow spherical structures (Fig. 5b), aggregates of small spheres (Fig. 5e) and discoidal structures (Fig. 5a, c–e). Additionally, samples contained long, slender needle-like forms with a groove down the middle (Fig. 5a, b, d, e). Although the needle-like forms are found throughout all samples, they are found in thick mats over Aix 13 (Fig. 5a). Similarly, although the discoid microfossils are found on the fossil bodies (Fig. 5c–e), they are most prevalent in the matrix (Fig. 5a). Like the long forms, these are found in isolation (Fig. 5c–e) as well as in thicker mats (Fig. 5a).

**Energy-dispersive X-ray spectroscopy (EDS).** EDS was performed on some of the fossils and thin sections of the matrix. EDS reveals that the brown material found within the fossils is composed of co-located S and C (Fig. 6). In all samples, the matrix around the fossil as well as areas within the fossil not composed of the brown material are composed of Si, which is found co-located with O (Figs. 2c and 6). Ca is also found throughout the matrix (Fig. 6). The petrographic thin sections cut



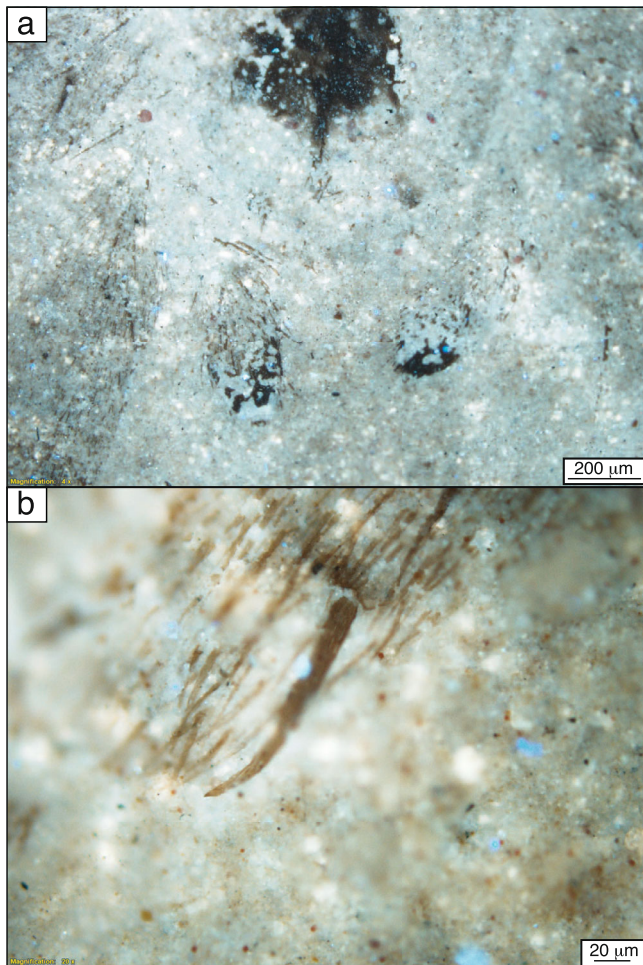


**Fig. 3 UV illumination revealing preservation of morphological details on spider fossil.** Fossil Aix\_PS4 shown under UV illumination. Autofluorescence of the fossil material reveals morphological details like the spider's pedipalps (a) and setae and claw (b).

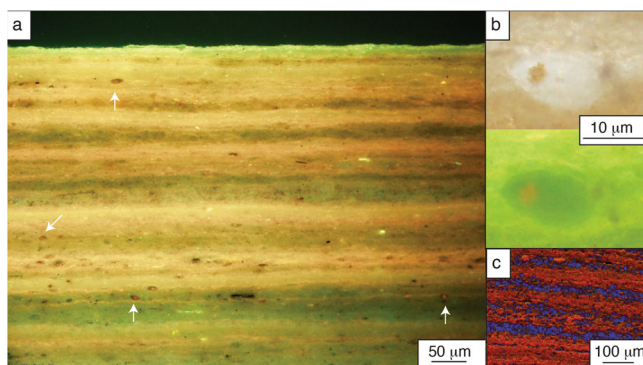


**Fig. 4 Cross section of matrix around fossils seen in plain light, UV illumination, and analyzed by energy-dispersive x-ray spectroscopy.** a When illuminated by UV light, matrix autofluoresces yellow and green, revealing thin laminae. Matrix is also marked by small microfossils with a red spot; four of these features are marked by white arrows. b Close-up of one of these features, as seen under plain light (top) and UV illumination (bottom). Under plain light, these microfossils are mainly clear with a denser spot; under UV illumination that spot autofluoresces red. c Chemical composition of the matrix, revealing that the laminations are alternately Si-rich (red, thicker laminae) and Ca-rich (blue). This also reveals that the microfossils are composed of Si, as seen by the two oblong bodies near the top of the image.

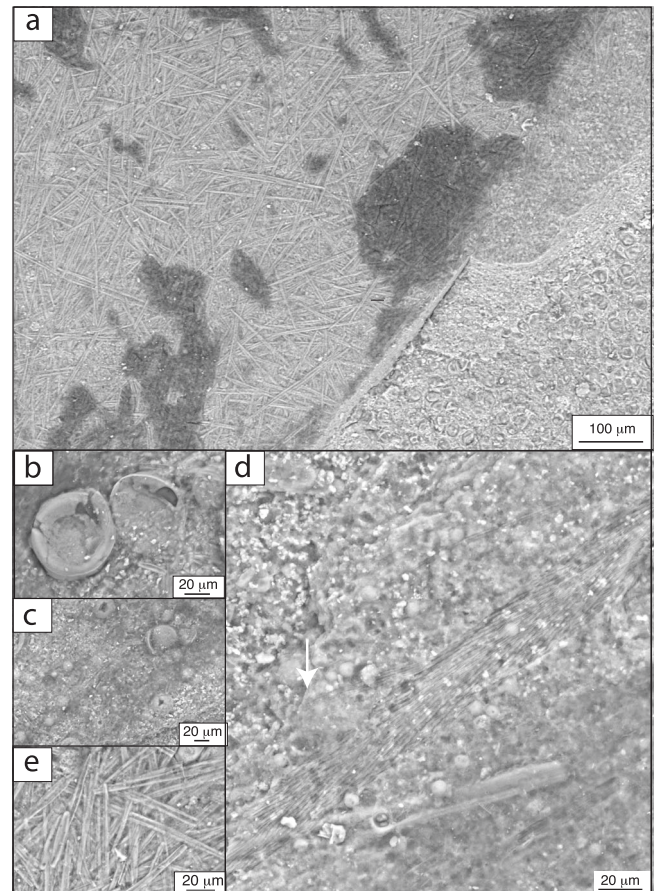


**Fig. 5 SEM images of microfossils and black draping polymer.** a Aix\_13, showing pennate diatoms over the body of the spider and centric diatoms in the matrix surrounding the body of the spider, as well as the black polymer that drapes over the pennate diatoms. b Two large microfossils within Aix\_17' with semicircular apertures overlying pennate and centric diatoms. c Black polymer in Aix\_17 draping over centric diatoms. d Aix\_17, showing black polymer draping over pennate and centric diatoms. Sample also contains imprint of the setae found on the spider's leg, at white arrow. e Aix\_13, magnified view of thick pennate diatom mats, also showing centric diatom in the top right corner and a clustered microfossil that resembles a chrysophyte in top left corner.

perpendicular through the matrix revealed the laminations are composed of alternating layers of Ca and Si (Fig. 4c).

The resolution of the EDS data is such that they can be correlated with the microfossils visible in the SEM. This correlation reveals that the discoid microfossils and the needle-like microfossils are composed of silica (Fig. 7a, b).

## Discussion

Correlating SEM imaging with EDS analysis and fluorescent microscopy reveals that these spiders are preserved as a carbon-sulfur complex in a siliceous microfossil-rich environment. The hollow structures and the aggregates resemble the stomatocysts of golden-brown algae (Chrysophyta)<sup>37–40</sup>, while the other siliceous fossils are likely centric and pennate diatoms. The morphology and the low diversity of the pennate diatoms suggests that these are likely planktonic diatoms<sup>41</sup>. This identification is supported by the fluorescence microscopy data, as chlorophyll degradation products from diatom chloroplasts autofluoresce red under UV illumination (Fig. 4b)<sup>42</sup>. Similarly, correlating the SEM microscopy with the EDS chemical data reveals that the fossils



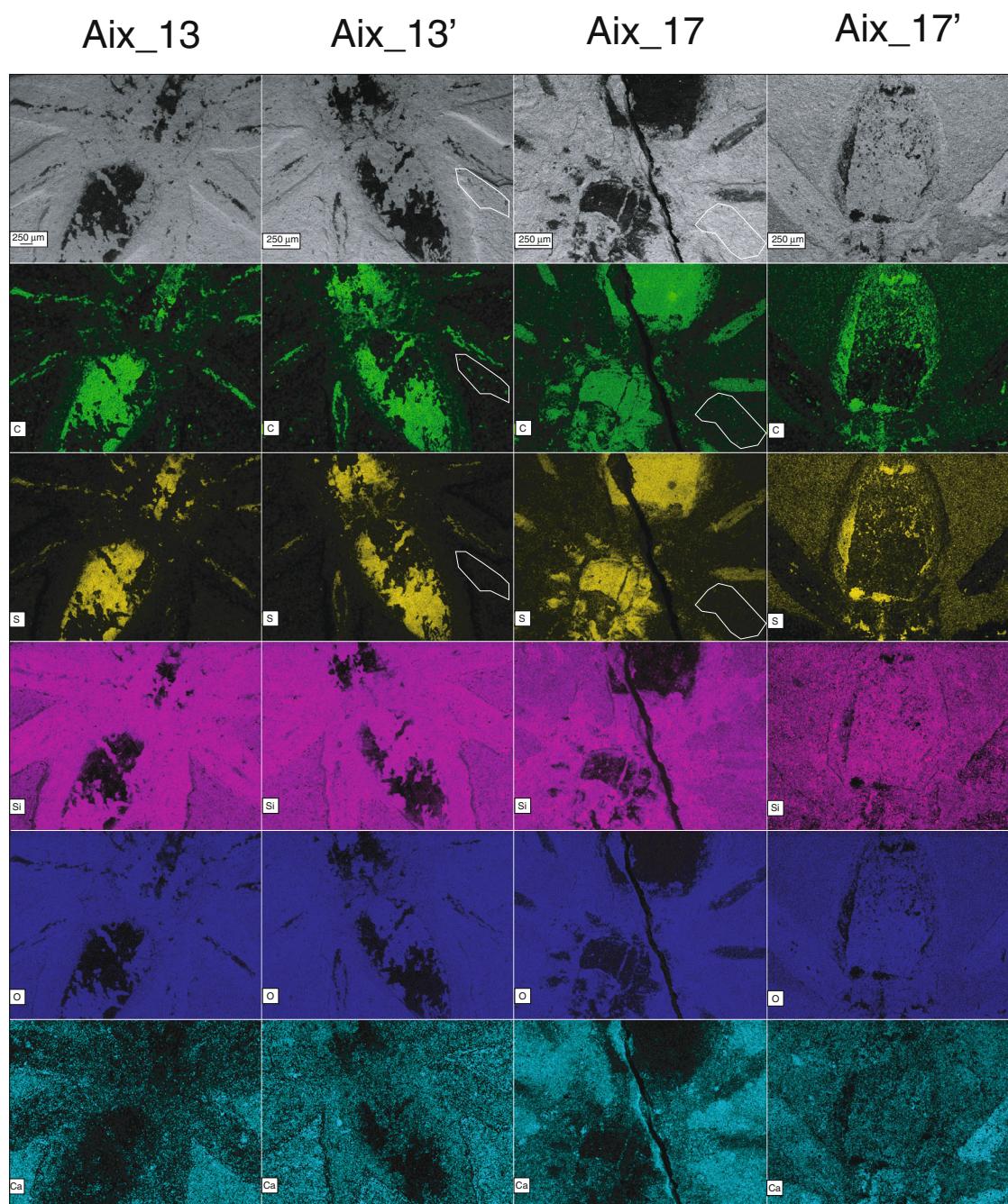


**Fig. 6 Chemical maps of part and counterpart of two spider fossils from the Aix-en-Provence Formation.** Part and counterpart of samples Aix\_13 and Aix\_17 showing distribution of, from top to bottom, C, S, Si, O, and Ca. The chemical maps reveal that C and S are co-located in areas of the fossil where the black polymer is located, that both the matrix and the spider fossils contain co-located Si and O, and the matrix contains Ca. White circles indicate two example areas where C in the matrix is not associated with S, demonstrating the two elements are co-located on the body of the spider fossil.

preserve a carbon and sulfur-rich polymer. This polymer auto-fluoresces yellow and orange, providing a relatively straightforward way to detect these areas in other fossils.

These two factors speak to a potential taphonomic pathway for preserving these arachnids in the Aix-en-Provence Formation: sulfurization. Sulfurization, or natural vulcanization, is an abiotic organic carbon polymerization process initiated by the production of sulfides by sulfate reducing microbes. It is thought that most of the organically bound sulfur in the geosphere is the result of this diagenetic process, which has been observed to occur within hours to days and at low temperatures<sup>43–47</sup>. The chemical reactions that

result in sulfur cross-linkages between organic molecules, stabilizing and preserving the organic material are well characterized, as is the fact that microbial reduction of sulfate is a key process in providing sulfide for this chemical reaction<sup>43,46,48–53</sup>. Sulfurization requires a ready source of sulfate compounds, which once transformed into sulfide, cross link organic compounds or react with appropriately functionalized bonds in already present biopolymers<sup>43</sup>. The resulting polymer is quite resistant to degradation, as the carbon is no longer easily bioavailable and is stable<sup>43,54</sup>. Studies have shown that this type of naturally vulcanized compound can be preserved in the rock record for millions of years<sup>50,55</sup>.



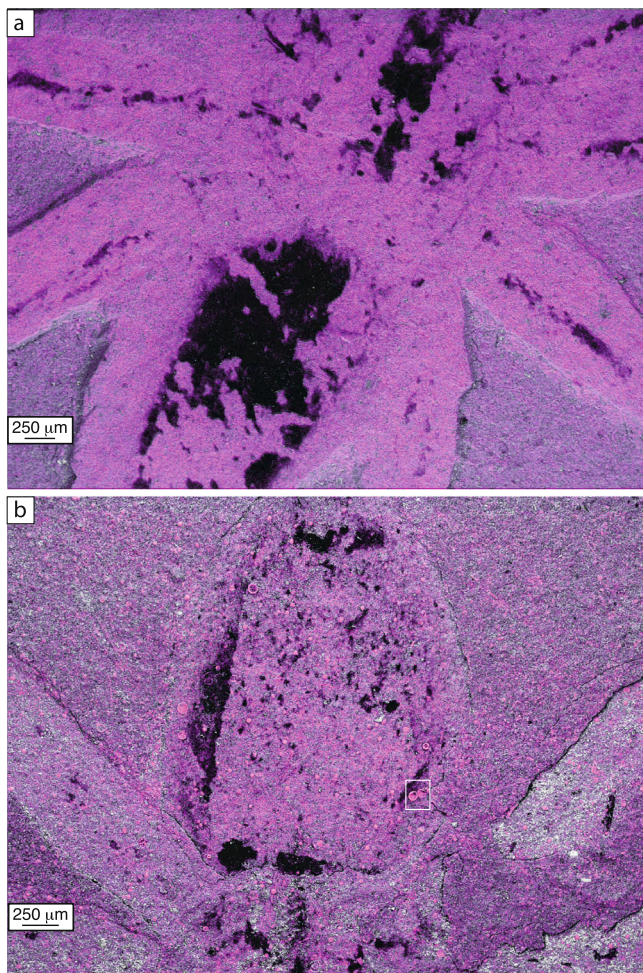


**Fig. 7** Si elemental map overlaid on SEM images of two fossil spiders. Superimposed EDS map on **a** Aix\_13 and **b** Aix\_17' revealing that the microfossils are composed of silica. Box in **b** shows microfossils visible in Fig. 5b.

Sulfurization is a chemical reaction that occurs in anoxic environments with a supply of hydrogen sulfide<sup>43–47</sup>. Previously, it has been suggested that diatom EPS could aid fossil preservation by generating an anaerobic environment<sup>6–8</sup>, but this appears to only be half the necessary mechanism: diatom EPS is also rich in sulfate and sulfonate esters<sup>25–27</sup>, compounds shown to be a major substrate for sulfate-reducing bacteria<sup>56,57</sup> (Fig. 8b). Thus, although the anaerobic environment within a diatom mat can help facilitate preservation, the diatom EPS also acts as a source of sulfate, both of which are necessary to drive sulfurization. Although the Aix-en-Provence Formation contains gypsum-rich intervals, indicating that this environment was periodically enriched in sulfate<sup>34</sup>, there is no evidence for sulfate precipitation in the matrix surrounding the fossils (Figs. 2 and 7).

When an insect or spider becomes entrapped in a diatomaceous mat, the EPS from the diatom community would quickly cover the organism<sup>6,8,58</sup> (Fig. 8). Additionally, the mass of EPS around the spider could allow for rapid particle sinking if the mat is planktonic, bringing the organism down to the sediment/water interface<sup>46</sup>. Spider exoskeletons are composed of chitin, a polysaccharide, along with proteins and glycoproteins<sup>59,60</sup>, a complex sometimes referred to as arthropodin<sup>61,62</sup>. The chitin-protein complexes of a spider are cross linked with metal ions, and the epicuticle of a spider is coated in wax<sup>59,63</sup>. Chitin is the second most abundant biopolymer on Earth, and has been found in a

myriad of taxonomic groups, including fungus, algae, sponges, protists, insects, molluscs, crustaceans, reptiles, and amphibians<sup>64,65</sup>. This biopolymer is composed of chains of N-acetylglucosamine and, in most organisms, including spiders, chitin is synthesized as  $\alpha$ -chitin, consisting of microfibrils of about twenty chitin chains arranged antiparallel to one another<sup>64,65</sup> (Fig. 8a). The N-acetylglucosamine monomer contains a carbonyl group; in  $\alpha$ -chitin, due to the antiparallel configuration, the carbonyl groups on different chains are located near one another (Fig. 8a). Carbonyl groups, along with conjugated double bonds, have been shown to be the strongest acceptors for polysulfide addition in sulfurization reactions<sup>47,53,66</sup>. Furthermore, these S-functionalities can react with nearby molecules, producing secondary intermolecular S–S cross linkages<sup>47,49</sup> (Fig. 8c). Thus, the chemical structure of chitin makes it very well suited to act as a substrate for sulfurization reactions (Fig. 8c). Although the protein complexes<sup>59</sup> and waxes do not provide as many reaction sites<sup>63</sup>, it is possible that they also could make a more minor contribution to sulfurization<sup>67,68</sup>. The fact that these C–S complexes are only found in association with the spider morphology indicates that it is likely that the spiders are the source of the organic material involved in sulfurization. For instance, EDS analysis reveals C-rich areas in the matrix surrounding the fossils, but they are not associated with S (Fig. 6). As diagenesis continues, with burial and increasing thermal maturity, the spider is likely to experience flattening<sup>69</sup>, and, at an atomic level, these newly formed C–S and S–S bonds are likely to be further rearranged to more stable bonds, such as aromatic carbon bonds<sup>47,53</sup> (Fig. 8d).

Previously, two mechanisms had been described for preserving spiders in sedimentary environments: kerogenization and mineralization<sup>69</sup>. Authigenic mineralization preserves soft-bodied organisms, sometimes with high levels of fidelity, by replicating the structure of soft tissues through the formation of minerals such as calcite, apatite, and pyrite<sup>70</sup>. Pyritization occurs through microbial sulfate reduction in low oxygen conditions with an abundance of sulfate and iron and low organic carbon concentrations<sup>71</sup>. Pyritization is rare in freshwater lacustrine settings due to a relatively low concentration of sulfates<sup>4</sup>. Kerogenization is the general name given to preserving cuticle remains as compression fossils consisting of only a thin layer of carbonized material and possibly very low relief impressions<sup>69</sup>. The fidelity of fossil preservation of cuticular remains varies from locality to locality, perhaps due to the environmental conditions of deposition. Kerogenization is described as the process by which the cuticle of spiders is altered during diagenesis to either aliphatic or aromatic compounds<sup>69</sup>, and is thought to be due to the polymerization of free and ester-bound cuticular lipids<sup>2</sup>. Sulfurization would provide a possible chemical pathway by which this polymerization could occur.

If the entombment of organisms in diatom mats is a major pathway to preservation, it should be fairly widespread across the Cenozoic. We augmented a previously published list of exceptional fossil localities<sup>1</sup> with additional sites found in the literature. Examining the Cenozoic localities for the presence of diatoms revealed that diatomaceous units represent a substantial proportion of all of the exceptionally preserved fossil sites through this time period (Fig. 9, Table 1, and Supplementary Data 1). These localities are found globally (Fig. 9), and 70% of all reported Cenozoic Fossil-Lagerstätten localities are diatomaceous, a number that increases to 76% when the units that are likely, based on their descriptions, to contain diatoms, despite the fact that diatoms have not been reported from these units (Table 1 and Supplementary Data 1). Furthermore, in the Paleocene, before the diatoms fully invaded the continental realm<sup>10,11</sup>, diatom-rich deposits represent 29% of the deposits, as opposed to 82% in the

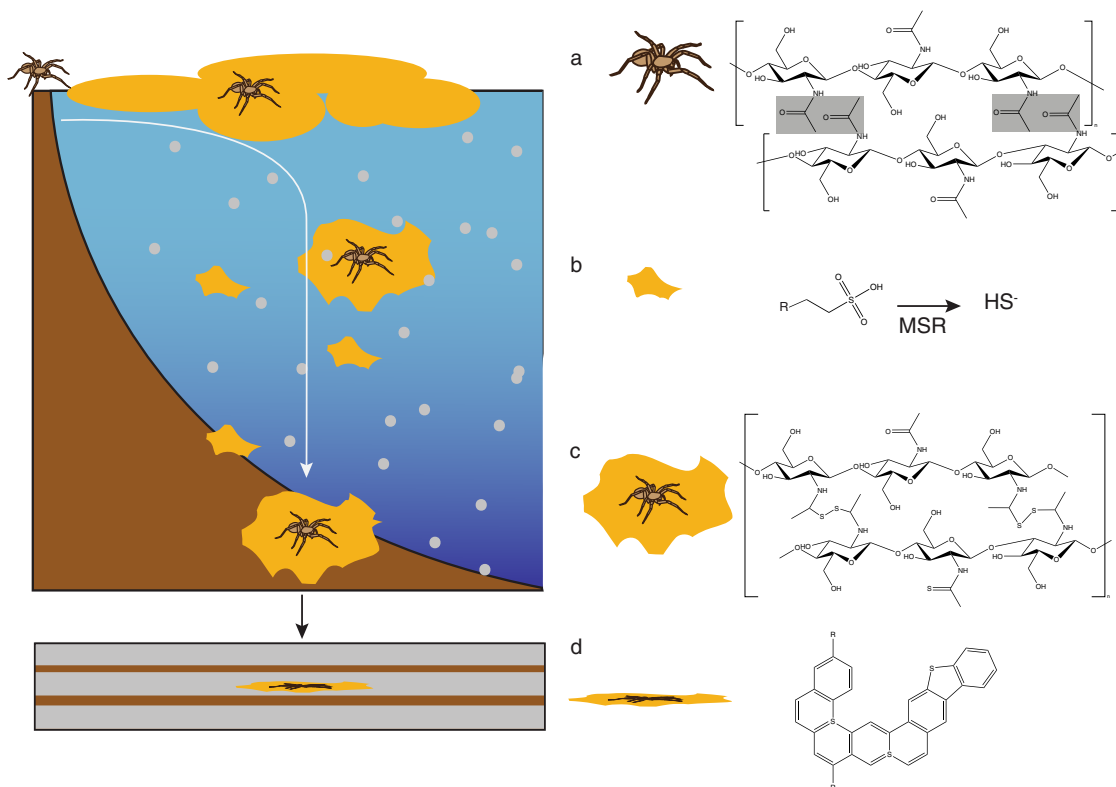


**Fig. 8 Proposed diatom-influenced taphonomic pathway.** Cartoon shows the entire proposed pathway: spider becomes entrained in planktonic diatom mat. Pieces of the diatom mat, both with and without spiders entrained within fall to the sediment floor against a background sedimentation of other diatoms and algae (gray dots). With time, these sediments become compressed and preserved into the rock record. **a** Chemical composition of chitin. Two chains of chitin are illustrated, organized in anti-parallel. Gray boxes indicate the carbonyl functionalities on the chitin. **b** Sulfonate-containing molecule, which are common in diatom EPS<sup>26,27</sup>, can undergo microbial sulfate reduction (MSR), leading to the production of sulfide. **c** Chitin molecule after sulfurization. C-S bonds could potentially replace the carbonyl functionalities, and S-S bridges could form across the chitin chains<sup>47,53,66</sup>. **d** Idealized molecule representing a chitin polymer after further diagenetic alteration, which could result in the formation of aromatized carbon<sup>53</sup>.

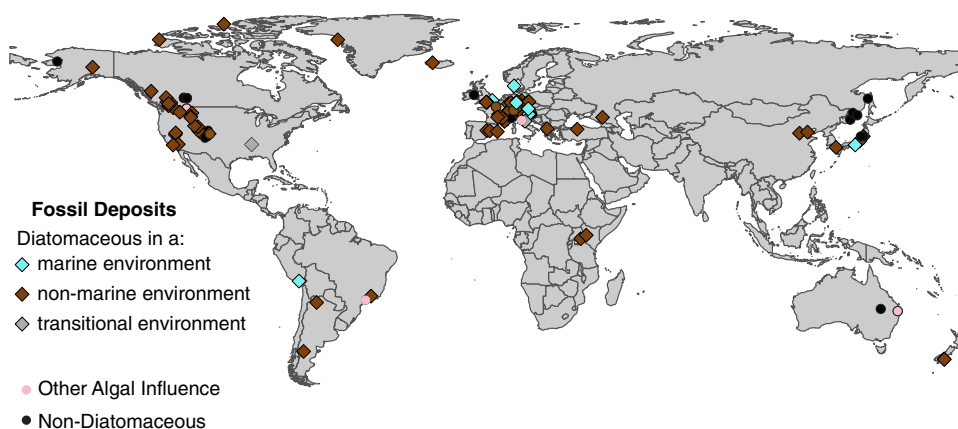


**Fig. 9 Map of 108 sites of exceptional fossil preservation identified across the Cenozoic, 76 of which are diatomaceous.** Sites where researchers have reported the presence of diatoms are mapped as diamonds and are divided by reported environment of deposition (marine, non-marine, or transitional). Non-diatomaceous sites are marked with circles, with black indicating no reported diatoms and pink reporting influence of other algae.

Miocene. This is striking as the co-occurrence of diatom fossils is likely underreported; many studies of these fossils are only done on the macroscopic scale, which would not necessarily reveal the presence of diatoms. As a prime example, to the best of our knowledge, this work is the first description of diatoms from the Aix-en-Provence Formation, despite its long history of investigation. This database also reveals that there are far more

exceptionally preserved fossil localities in non-marine environments than in marine or transitional environments, highlighting the invasion of the terrestrial realm by diatoms through the Cenozoic. This relationship between diatoms and Cenozoic sites with exceptional fossil preservation has not been noted before, although some studies have remarked on the abundance of diatoms present around the fossils<sup>5</sup>.



**Table 1 Sites of exceptional fossil preservation across the cenozoic divided into environment of deposition.**

	# Fossil Lagerstätten (# diatomaceous)	# of non-marine F-L (# diatomaceous)	# of transitional F-L (# diatomaceous)	# of marine F-L (# diatomaceous)
Pliocene	8 (5)	8 (5)	0 (-)	0 (-)
Miocene	34 (28)	27 (23)	2 (1)	5 (4)
Oligocene	26 (16)	24 (14)	0 (-)	2 (2)
Eocene	33 (25)	27 (21)	3 (2)	3 (2)
Paleocene	7 (2)	7 (2)	0 (-)	0 (-)

The chemistry of the spider fossils of the Aix-en-Provence Formation suggests that, as diatoms invaded the terrestrial realm throughout the Cenozoic, they might also have been inducing chemical polymerization of the organic carbon found in the insects, fish, amphibians, plants, and arachnids that lived in and around these lakes. Revisiting these other deposits with the same chemical and microscopic techniques used here could reveal if similar relationships are present in those localities. If true, this hitherto unknown taphonomic pathway would have allowed the preservation of many lacustrine fossils across the Cenozoic, informing our knowledge of the evolution of terrestrial life especially through this time period.

## Methods

**Materials.** This study uses eight fossil spiders, including three parts and counterpart pairs (Aix\_13 + 13', Aix\_17 + 17', Aix\_25 + 25', Aix\_PS4, Aix\_Flat1), from the Oligocene Aix-en-Provence, France, Fossil-Lagerstätte (43°31'48"N; 5°23'24"E). Specimens were loaned to PAS and are reposit in the National Museum of Natural History, Paris, France. The specimens had been glued to small pieces of notecard before this study began because the fossils are extremely thin and delicate.

**Microscopy and chemical analysis.** Fossils were photographed with a Canon EOS 5D Mark II digital camera attached to a copy stand and the same camera attached to a Leica M650C microscope and viewed in low angle light to enhance details not easily seen under direct light. Pieces of matrix material from five fossil specimens were embedded in epoxy to make thin sections. Thin sections were prepared in the Rock and Thin Section Preparation Lab at the University of Kansas. Fluorescence imaging was conducted with an Olympus BX51 Petrographic Scope equipped with a mercury vapor-arc-discharge lamp and two exciter filters transmitting in the UV (330–385 nm wavelength) and violet-blue (400–440 nm wavelength) regions. Whole fossil specimens were imaged using both wavelengths of light. Stacked and stitched images were created using Stream Essentials software. Scanning electron microscopy (SEM) and energy-dispersive x-ray spectroscopy (EDS) analyses were conducted at the University of Kansas Microscopy and Analytical Imaging Laboratory and the University of Missouri X-ray Microanalysis Core Facility. At the University of Kansas Microscopy and Analytical Imaging Laboratory, the Aix\_Flat1 fossil specimen and slide were sputter-coated with iridium and mounted on individual aluminum stubs with copper tape for image acquisition. Images and analyses were acquired on a Cold Field Emission SEM, Hitachi High Technologies, SU8230 series, with a YAB backscattered electron (BSE) detector, at accelerating voltages ranging from 1.0 to 2.0 keV. EDS used a Silicon Drift Detector to create elemental maps. The iridium coating does not hinder the elemental analyses. At University of Missouri X-ray Microanalysis Core Facility, samples Aix\_13 + 13', Aix\_17 + 17', Aix\_25 + 25', and Aix\_PS4 were analyzed uncoated, mounted directly to aluminum stage plates using copper tape, and analyzed using a field emission Zeiss Sigma 500VP. Beam and chamber conditions were as follows: low-vacuum chamber pressure = 25 Pa with a dry nitrogen (99.999%) atmosphere; sample working distance 9.5 mm ± 0.7 mm; beam accelerating voltage = 20 keV, beam current = 40 nA; 60 µm aperture. Imaging was conducted with a high-definition 5-segment backscatter detector and a cascade current low-vacuum secondary electron detector, including large-area image mosaics compiled using the ATLAS workflow (Fibics Inc.). EDS elemental mapping was conducted with dual, co-planar Bruker XFlash 6|30 SDD spectrometers used in tandem for 600 s live time.

## Data availability

The EDS and SEM images that support the findings of this study are available in figshare with the identifier <https://doi.org/10.6084/m9.figshare.19406654.v1> and the Supplementary Information file is available in figshare with the identifier <https://doi.org/10.6084/m9.figshare.19310669.v1>.

Received: 12 October 2021; Accepted: 24 March 2022;

Published online: 21 April 2022

## References

- Muscente, A. D. et al. Exceptionally preserved fossil assemblages through geologic time and space. *Gondwana Res.* **48**, 164–188 (2017).
- Stankiewicz, B. A. et al. Alternative origin of aliphatic polymer in kerogen. *Geology* **28**, 559–562 (2000).
- Seilacher, A. Begriff und Bedeutung der Fossil-Lagerstätten. *N. Jahrb. Geol. Paläont. Monatsh.* **1970**, 34–39 (1970).
- Allison, P. A. Konservat-Lagerstätten: cause and classification. *Paleobiology* **14**, 331–344 (1988).
- Briggs, D. E., Stankiewicz, B. A., Meischner, D., Bierstedt, A. & Evershed, R. P. Taphonomy of arthropod cuticles from Pliocene lake sediments, Willershausen, Germany. *Palaio* **13**, 386–394 (1998).
- O'Brien, N. R., Meyer, H. W., Reilly, K., Ross, A. M. & Maguire, S. Microbial taphonomic processes in the fossilization of insects and plants in the late Eocene Florissant Formation, Colorado. *Rocky Mt. Geol.* **37**, 1–11 (2002).
- Bustillo, M. Á., Talavera, R. R. & Sanchiz, B. Biomineralization and diagenesis in a Miocene tadpole: a mineralogical and taphonomic study. *J. Iber. Geol.* **45**, 609–624 (2019).
- O'Brien, N. R., Meyer, H. W. & Harding, I. C. The role of biofilms in fossil preservation, Florissant Formation, Colorado. *Paleontol. Upper Eocene Florissant Form. Colo.* **435**, 19 (2008).
- Decho, A. W. Microbial exopolymer secretions in ocean environments: their role (s) in food webs and marine processes. *Oceanogr. Mar. Biol. Annu. Rev.* **28**, 73–153 (1990).
- Girard, V. et al. Thai amber: insights into early diatom history? *BSGF Earth Sci. Bull.* **191**, 1–23 (2020).
- Sims, P. A., Mann, D. G. & Medlin, L. K. Evolution of the diatoms: insights from fossil, biological and molecular data. *Phycologia* **45**, 361–402 (2006).
- Siver, P. A. et al. *Aulacoseira giraffensis* (Bacillariophyceae), a new diatom species forming massive populations in an Eocene lake. *Plant Ecol. Evol.* **152**, 358–367 (2019).
- Siver, P. A., Wolfe, A. P. & Edlund, M. B. Taxonomic descriptions and evolutionary implications of Middle Eocene pennate diatoms representing the extant genera *Oxynesis*, *Actinella* and *Nupela* (Bacillariophyceae). *Plant Ecol. Evol.* **143**, 340–351 (2010).
- Kidder, D. L. & Gierlowski-Kordesch, E. H. Impact of grassland radiation on the nonmarine silica cycle and Miocene diatomite. *Palaio* **20**, 198–206 (2005).
- Kemp, A. E. S., Pike, J., Pearce, R. B. & Lange, C. B. The 'Fall dump'—a new perspective on the role of a 'shade flora' in the annual cycle of diatom production and export flux. *Deep Sea Res. Part 2* **47**, 2129–2154 (2000).
- Hayashi, T., Krebs, W. N., Saito-Kato, M. & Tanimura, Y. The turnover of continental planktonic diatoms near the middle/late Miocene boundary and their Cenozoic evolution. *PLoS ONE* **13**, e0198003 (2018).
- Rabosky, D. L. & Sorhannus, U. Diversity dynamics of marine planktonic diatoms across the Cenozoic. *Nature* **457**, 183–186 (2009).
- Wallace, A. R. *Regional Geologic Setting of Late Cenozoic Lacustrine Diatomite Deposits, Great Basin and Surrounding Region* (US Department of the Interior, US Geological Survey Bulletin 2209-B, 2003).
- Armbrust, E. V. The life of diatoms in the world's oceans. *Nature* **459**, 185–192 (2009).
- Chiovitti, A., Dugdale, T. M. & Wetherbee, R. in *Biological Adhesives* (eds Smith, A. M. & Callow, J. A.) 79–103 (Springer, 2006).
- Thornton, D. Diatom aggregation in the sea: mechanisms and ecological implications. *Eur. J. Phycol.* **37**, 149–161 (2002).
- Hoagland, K. D., Rosowski, J. R., Gretz, M. R. & Roemer, S. C. Diatom extracellular polymeric substances: function, fine structure, chemistry, and physiology. *J. Phycol.* **29**, 537–566 (1993).



23. Grossart, H.-P. & Simon, M. Limnetic macroscopic organic aggregates (lake snow): occurrence, characteristics, and microbial dynamics in Lake Constance. *Limnol. Oceanogr.* **38**, 532–546 (1993).
24. Grossart, H. P. & Simon, M. Bacterial colonization and microbial decomposition of limnetic organic aggregates (lake snow). *Aquat. Microb. Ecol.* **15**, 127–140 (1998).
25. Underwood, G. J. C. & Paterson, D. M. The importance of extracellular carbohydrate production by marine epipelagic diatoms. *Adv. Bot. Res.* **40**, 183–240 (2003).
26. Wustman, B. A., Gretz, M. R. & Hoagland, K. D. Extracellular matrix assembly in diatoms (Bacillariophyceae) (I. A model of adhesives based on chemical characterization and localization of polysaccharides from the marine diatom *Achnanthes longipes* and other diatoms). *Plant Physiol.* **113**, 1059–1069 (1997).
27. Huntsman, S. A. & Sloneker, J. H. An exocellular polysaccharide from the diatom *Gomphonema olivaceum*. *J. Phycol.* **7**, 261–264 (1971).
28. McConville, M. J., Wetherbee, R. & Bacic, A. Subcellular location and composition of the wall and secreted extracellular sulphated polysaccharides/ proteoglycans of the diatom *Stauroneis amphioxys* Gregory. *Protoplasma* **206**, 188–200 (1999).
29. Bellinger, B. J., Underwood, G. J. C., Ziegler, S. E. & Gretz, M. R. Significance of diatom-derived polymers in carbon flow dynamics within estuarine biofilms determined through isotopic enrichment. *Aquat. Microb. Ecol.* **55**, 169–187 (2009).
30. Nichols, C. M. et al. Chemical characterization of exopolysaccharides from Antarctic marine bacteria. *Microb. Ecol.* **49**, 578–589 (2005).
31. Callow, R. H. T. & Brasier, M. D. Remarkable preservation of microbial mats in Neoproterozoic siliciclastic settings: implications for Ediacaran taphonomic models. *Earth Sci. Rev.* **96**, 207–219 (2009).
32. Hope, F. W. XXXIX Observations on the fossil insects of Aix in Provence, with descriptions and figures of three species. *Trans. R. Entomol. Soc. Lond.* **4**, 250–255 (1847).
33. Nury, D. L'Oligocène de Provence méridionale: Stratigraphie, dynamique sédimentaire, reconstitutions paléogéographiques. (Doctoral Dissertation, Aix-Marseille 1, 1987).
34. Gaudant, J., Nel, A., Nury, D., Vêran, M. & Carnevale, G. The uppermost Oligocene of Aix-en-Provence (Bouches-du-Rhône, Southern France): a Cenozoic brackish subtropical Konservat-Lagerstätte, with fishes, insects and plants. *C. R. Palevol* **17**, 460–478 (2018).
35. Châteauneuf, J. J. & Nury, D. La flore de l'Oligocène de Provence méridionale: implications stratigraphiques, environnementales et climatiques. *Géol. de la France* **2**, 43–55 (1995).
36. Saporta, G. D. Dernières adjonctions à la flore fossile d'Aix-en-Provence. *Ann. Sci. Nat. Bot.* **10**, 1–192 (1889).
37. De Hoyos, C., Aldasoro, J. J., Toro, M. & Comín, F. A. *Phytoplankton and Trophic Gradients* 287–295 (Springer, 1998).
38. Siver, P. A. & Wolfe, P. A. Scaled chrysophytes in Middle Eocene lake sediments from Northwestern Canada, including descriptions of six new species. *Nova Hedwig. Beih.* **128**, 295–308 (2005).
39. Holen, D. A. Chrysophyte stomatocyst production in laboratory culture and descriptions of seven cyst morphotypes. *Phycologia* **53**, 426–432 (2014).
40. Siver, P. A. Remarkably preserved cysts of the extinct synurophyte, *Mallomonas amplia*, uncovered from a 48 Ma freshwater Eocene lake. *Sci. Rep.* **10**, 5204 (2020).
41. Patil, J. S. & Anil, A. C. Biofilm diatom community structure: influence of temporal and substratum variability. *Biofouling* **21**, 189–206 (2005).
42. Stasiuk, L. D. & Sanei, H. Characterization of diatom-derived lipids and chlorophyll within Holocene laminites, Saanich Inlet, British Columbia, using conventional and laser scanning fluorescence microscopy. *Org. Geochem.* **32**, 1417–1428 (2001).
43. Sinninghe Damsté, J. S. & De Leeuw, J. W. Analysis, structure and geochemical significance of organically-bound sulphur in the geosphere: state of the art and future research. *Org. Geochem.* **16**, 1077–1101 (1990).
44. Raven, M. R., Sessions, A. L., Adkins, J. F. & Thunell, R. C. Rapid organic matter sulfurization in sinking particles from the Cariaco Basin water column. *Geochim. Cosmochim. Acta* **190**, 175–190 (2016).
45. Tribouillard, N. et al. Storm-induced concentration of sulfurized, marine-origin, organic matter as a possible mechanism in the formation of petroleum source-rock. *Mar. Pet. Geol.* **109**, 808–818 (2019).
46. Raven, M. R., Keil, R. G. & Webb, S. M. Microbial sulfate reduction and organic sulfur formation in sinking marine particles. *Science* <https://doi.org/10.1126/science.abc6035>. (2021).
47. Raven, M. R., Keil, R. G. & Webb, S. M. Rapid, concurrent formation of organic sulfur and iron sulfides during experimental sulfurization of sinking marine particles. *Glob. Biogeochem. Cycles* **35**, e2021GB007062 (2021).
48. Werne, J. P. et al. Investigating pathways of diagenetic organic matter sulfurization using compound-specific sulfur isotope analysis. *Geochim. Cosmochim. Acta* **72**, 3489–3502 (2008).
49. Werne, J. P., Hollander, D. J., Lyons, T. W. & Damsté, J. S. S. Organic sulfur biogeochemistry: recent advances and future research directions. *Geol. Soc. Am. Spec. Pap.* **379**, 135–150 (2004).
50. McNamara, M. E., van Dongen, B. E., Lockyer, N. P., Bull, I. D. & Orr, P. J. Fossilization of melanosomes via sulfurization. *Palaeontology* **59**, 337–350 (2016).
51. Gupta, N. S. et al. Molecular preservation of plant and insect cuticles from the Oligocene Enspel Formation, Germany: evidence against derivation of aliphatic polymer from sediment. *Org. Geochem.* **38**, 404–418 (2007).
52. van Dongen, B. E., Schouten, S. & Sinninghe Damsté, J. S. Preservation of carbohydrates through sulfurization in a Jurassic euxinic shelf sea: examination of the Blackstone Band TOC cycle in the Kimmeridge Clay Formation, UK. *Org. Geochem.* **37**, 1052–1073 (2006).
53. Kutuzov, I., Rosenberg, Y. O., Bishop, A. & Amrani, A. in *Hydrocarbons, Oils and Lipids: Diversity, Origin, Chemistry and Fate* (ed. Wilkes, H.) 355–408 (Springer, 2020).
54. Grice, K., Schouten, S., Nissenbaum, A., Charrach, J. & Sinninghe Damsté, J. S. A remarkable paradox: sulfurised freshwater algal (*Botryococcus braunii*) lipids in an ancient hypersaline euxinic ecosystem. *Org. Geochem.* **28**, 195–216 (1998).
55. Lepot, K. et al. Organic matter heterogeneities in 2.72Ga stromatolites: alteration versus preservation by sulfur incorporation. *Geochim. Cosmochim. Acta* **73**, 6579–6599 (2009).
56. Visscher, P. T., Gritzer, R. F. & Leadbetter, E. R. Low-molecular-weight sulfonates, a major substrate for sulfate reducers in marine microbial mats. *Appl. Environ. Microbiol.* **65**, 3272–3278 (1999).
57. Cook, A. M., Laue, H. & Junker, F. Microbial desulfonation. *FEMS Microbiol. Rev.* **22**, 399–419 (1998).
58. Shear, W. A., Selden, P. A. & Gall, J.-C. Millipedes from the Grès à Voltzia, Triassic of France, with comments on Mesozoic millipedes (Diplopoda: Helminthomorpha: Eugnatha). *Int. J. Myriap.* **2**, 1–13 (2009).
59. Politi, Y., Bertinetti, L., Fratzl, P. & Barth, F. G. The spider cuticle: a remarkable material toolbox for functional diversity. *Philos. Trans. A Math. Phys. Eng. Sci.* **379**, 20200332 (2021).
60. Gibbons, A. T. et al. Amblypygid-fungal interactions: The whip spider exoskeleton as a substrate for fungal growth. *Fungal Biol.* **123**, 497–506 (2019).
61. Wigglesworth, V. B. The physiology of insect cuticle. *Annu. Rev. Entomol.* **2**, 37–54 (1957).
62. Willis, J. H., Regier, J. C. & Debrunner, B. A. in *Current Topics in Insect Endocrinology and Nutrition: A Tribute to Gottfried S. Fraenkel* (eds. Bhaskaran, G. et al.) 27–46 (Springer, 1981).
63. Chinta, S. P., Goller, S., Uhl, G. & Schulz, S. Identification and synthesis of branched wax-type esters, novel surface lipids from the spider *Argyodes elevatus* (Araneae: Theridiidae). *Chem. Biodivers.* **13**, 1202–1220 (2016).
64. Machalowski, T., Amemiya, C. & Jesionowski, T. Chitin of Araneae origin: structural features and biomimetic applications: a review. *Appl. Phys. A* **126**, 1–17 (2020).
65. Merzendorfer, H. The cellular basis of chitin synthesis in fungi and insects: common principles and differences. *Eur. J. Cell Biol.* **90**, 759–769 (2011).
66. Amrani, A. & Aizenshtat, Z. Mechanisms of sulfur introduction chemically controlled:  $\delta^{34}\text{S}$  imprint. *Org. Geochem.* **35**, 1319–1336 (2004).
67. Sinninghe Damsté, J. S., Kok, M. D., Köster, J. & Schouten, S. Sulfurized carbohydrates: an important sedimentary sink for organic carbon? *Earth Planet. Sci. Lett.* **164**, 7–13 (1998).
68. Kok, M. D., Schouten, S. & Sinninghe Damsté, J. S. Formation of insoluble, nonhydrolyzable, sulfur-rich macromolecules via incorporation of inorganic sulfur species into algal carbohydrates. *Geochim. Cosmochim. Acta* **64**, 2689–2699 (2000).
69. Martínez-Delclòs, X., Briggs, D. E. G. & Peñalver, E. Taphonomy of insects in carbonates and amber. *Palaeogeogr. Palaeoclimatol. Palaeoecol.* **203**, 19–64 (2004).
70. Briggs, D. E. G. The role of decay and mineralization in the preservation of soft-bodied fossils. *Annu. Rev. Earth Planet. Sci.* **31**, 275–301 (2003).
71. Briggs, D. E. G., Raiswell, R., Bottrell, S. H., Hatfield, D. & Bartels, C. Controls on the pyritization of exceptionally preserved fossils: an analysis of the Lower Devonian Hunsrück Slate of Germany. *Am. J. Sci.* **296**, 633–663 (1996).

## Acknowledgements

The authors thank André Nel (National Museum of Natural History, Paris, France) for loaning the specimens, Prem S. Thapa-Chettri at the Microscopy and Analytical Imaging Laboratory at the University of Kansas for electron microscopy of selected samples, Gregory Druschel for helpful discussion, the Evolving Earth Foundation for funding to M.R.D., and three anonymous reviewers for constructive feedback. The University of Missouri X-ray Microanalysis Core Facility was supported by NSF IF #1636643 to J.D.S.

## Author contributions

The authors confirm contribution to the paper as follows. A.N.O.: study conception and design, data collection, analysis and interpretation of results, draft manuscript preparation; M.R.D.: study conception and design, data collection, analysis and interpretation of results; J.D.S.: study conception and design, data collection; P.A.S.: study conception and design, sample acquisition. All authors reviewed the results and approved the final version of the manuscript.

## Competing interests

The authors report no competing interests.

## Additional information

**Supplementary information** The online version contains supplementary material available at <https://doi.org/10.1038/s43247-022-00424-7>.

**Correspondence** and requests for materials should be addressed to Alison N. Olcott.

**Peer review information** *Communications Earth & Environment* thanks Morgan Reed Raven, Jeffery Stone and the other, anonymous, reviewer(s) for their contribution to the peer review of this work. Primary Handling Editor: Joe Aslin.

**Reprints and permission information** is available at <http://www.nature.com/reprints>

**Publisher's note** Springer Nature remains neutral with regard to jurisdictional claims in published maps and institutional affiliations.



**Open Access** This article is licensed under a Creative Commons Attribution 4.0 International License, which permits use, sharing, adaptation, distribution and reproduction in any medium or format, as long as you give appropriate credit to the original author(s) and the source, provide a link to the Creative Commons license, and indicate if changes were made. The images or other third party material in this article are included in the article's Creative Commons license, unless indicated otherwise in a credit line to the material. If material is not included in the article's Creative Commons license and your intended use is not permitted by statutory regulation or exceeds the permitted use, you will need to obtain permission directly from the copyright holder. To view a copy of this license, visit <http://creativecommons.org/licenses/by/4.0/>.

© The Author(s) 2022